ARTICLE

Ab Initio Calculation on Spectroscopic Properties and Radiative Lifetimes of Low-Lying Excited States of NaK

Shi-yang Zhang[a], Feng Xie[b], Feng-dong Jia[a], Xiao-kang Li[a], Ru-quan Wang[c], Rui Li[d,e], Yong Wu[d*], Zhi-ping Zhong[a,f*]

a. School of Physics, University of Chinese Academy of Sciences, Beijing 100049, China
b. Institute of Nuclear and New Energy Technology, Collaborative Innovation Center of Advanced Nuclear Energy Technology, Key Laboratory of Advanced Reactor Engineering and Safety of Ministry of Education, Tsinghua University, Beijing 100084, China
c. Institute of Physics, Chinese Academy of Sciences, Beijing 100190, China
d. Data Center for High Energy Density Physics, Institute of Applied Physics and Computational Mathematics, Beijing 100088, China
e. Department of Physics, College of Science, Qiqihar University, Qiqihar 161006, China
f. CAS Center for Excellence in Topological Quantum Computation, University of Chinese Academy of Sciences, Beijing 100190, China

(Dated: Received on April 1, 2019; Accepted on July 15, 2019)

We performed high-level *ab initio* calculations on electronic structure of NaK. The potential energy curves (PECs) of 10 Λ-S states correlated with the three lowest dissociation limits have been calculated. On the basis of the calculated PECs, the spectroscopic constants of the bound Λ-S states are obtained, which are in good agreement with experimental results. The maximum vibrational quantum numbers of the singlet ground state $X^1\Sigma^+$ and the triplet ground state $a^3\Sigma^+$ have been analyzed with the semiclassical scattering theory. Transition properties including transition dipole moments, Franck-Condon factors, and radiative lifetimes have been investigated. The research results indicate that such calculations can provide fairly reliable estimation of parameters for the ultracold alkali diatomic molecular experiment.

Key words: Ultracold dipolar molecule, Transition dipole moment, Spectroscopic constants, Potential curves

I. INTRODUCTION

Ultracold polar molecules with their long-range electric dipolar interactions, many internal degrees (electronic, vibrational, and rotational degrees of freedom), low temperatures and long lifetimes, promise a novel platform in a wide range of areas for studying correlated quantum many-body phenomena, *e.g.*, a novel platform for quantum state resolved chemistry [1], precision measurements of fundamental constants [2–4], quantum computation [5], quantum simulation [6, 7]. Currently, the most successful experimental pathways of producing ultrapolar molecules can be divided into two main steps [8]: (i) the formation of weakly bound molecules by association of a pair of ultracold atoms via a Feshbach resonance, (ii) coherently transferred into the absolute rovibrational ground state via a two-photon stimulated Raman adiabatic passage (STIRAP) by means of avoided crossings or radio-frequency transitions. STIRAP is based on a so-called Lambda scheme of energy levels: the population is transferred from an initial level $|\mathrm{i}\rangle$ (usually referred to as a Feshbach molecule/Fano-Feshbach resonance mixed singlet and triplet symmetries) to a final level $|\mathrm{g}\rangle$ via an intermediate level $|\mathrm{e}\rangle$ (the $|\mathrm{e}\rangle$ levels possessing noticeable dipole-allowed transition probabilities with both $|\mathrm{i}\rangle$ and $|\mathrm{g}\rangle$). To realize transfer with high efficiency from weakly bound Feshbach molecules to the absolute ground state needs a properly designed two-photon stimulated Raman process. High-precision *ab initio* calculations can provide reliable estimation of important physical parameters, including (i) accurate Born-Oppenheimer potentials for the ground and excited states, (ii) the maximum bound states of the ground singlet state and triplet state in order to obtain proper Fano-Feshbach resonance states, (iii) the laser wavelength range for the two transitions from the initial Feshbach state to the intermediate state and from the intermediate state to the molecular ground state.

The diatomic heteronuclear alkali-metal molecules are an ideal candidate system for ultracold polar molecules, due to the easy realization of ultracold alkali atoms and the large permanent electric dipole mo-

*Authors to whom correspondence should be addressed.
E-mail: zpzhong@ucas.ac.cn, wu_yong@iapcm.ac.cn

DOI:10.1063/1674-0068/cjcp1904065

ment. Recently, Yang *et al.* [9] detected magnetically tunable Feshbach resonances in ultracold collisions between the ground state of NaK molecules and K atoms. Hartmann *et al.* [10] carried out a detailed investigation of Feshbach resonances in Na+K mixtures and provided refined potential curves for the NaK molecule. However, comprehensive account of scattering and near-threshold properties is still lacking [11], and there exists a significant gap between the highest observed vibrational levels and the asymptotic region where the Feshbach resonances take place [12].

Due to the chemical stablility of the ground state, NaK molecule is chosen by most experimental groups. In 2015, Zwierlein *et al.* [13] firstly realized the nearly quantum degenerate ultracold NaK gas and transformed the Feshbach molecule to the absolute ground state of NaK with a 75% transfer efficiency. Our current study on the NaK molecule attempts to describe the electronic structures and spectroscopic properties of the excited states of the alkali diatomic molecules by using high-level *ab initio* calculations, and provides reliable information about the Fano-Feshbach resonance state and the laser wavelengths used in the STIRAP experiment.

Alkali dimers can be treated as systems with two active electrons moving in a field of two ionic cores, and the core-polarization effect and core penetration effect are very notable in the alkali atoms. The results from the traditional high-precision quantum calculation method such as configuration interaction (CI) method even dealing with the low excited states of Na atom, K atom, or their molecules, will exhibit a large deviation from the experimental data. In 1984, Meyer *et al.* [14] simply added a semi-empirical core polarization potential to the valence electrons Hamiltonian. A cutoff function is then introduced to deal with the interaction effects in short range, and to overcome computational difficulties. The deviations of the harmonic frequency ω_e and the dissociation energy D_e of the ground state between theoretical calculations and experimental data are 1 cm^{-1} and 100 cm^{-1}, respectively. In the framework of pseudopotential methods, Jeung *et al.* [15–17] calculated the potential curves of 9 Λ-S states of the NaK molecule. The average deviations of the equilibrium internuclear distance R_e, the minimum of the potential curve T_e, the harmonic frequency ω_e, and the dissociation energy D_e of these states are 0.18 a_0, 491 cm^{-1}, 5.48 cm^{-1}, and 481 cm^{-1}, as compared to the experimental values. In 1996, Magnier *et al.* [18] systematically analyzed the potential energy curves (PECs) of the ground state and excited states of the NaK molecule in the framework of pseudopotential model, including 14 Σ^+ states, 10 Π states, and 5 Δ states. The different cutoff parameters of ρ_s, ρ_p, ρ_d, and ρ_f, *etc.*, have been set according to the individual atomic orbit, which are more accurate than those obtained by the single cutoff parameter method used by Meyer [12]. These calculated deviations from the experimental values for R_e, T_e, ω_e, and D_e of the 9 Λ-S states decreased to 0.04 a_0, 46 cm^{-1}, 1.24 cm^{-1}, and 72 cm^{-1}, respectively. In 2000, Magnier *et al.* [19] extended the quantum calculation range, including 17 Σ^+ states, 13 Π states, and 7 Δ states, and provided permanent electric dipole moment and transition dipole moment (TDM) of partial excited states. They also presented the severe distortion of the PECs of the $B^1\Pi$ and $b^3\Pi$ states for the strong interaction leading to the avoided crossing in short range and ionic covalent bond interaction in long range. In experiment, rovibrational energy levels and partial hyperfine structure of the singlet state and triplet state including $X^1\Sigma^+$, $a^3\Sigma^+$, $A^1\Sigma^+$, $b^3\Pi$, $c^3\Sigma^+$, $B^1\Pi$, *etc.*, have been determined. A number of measurements by laser induced fluorescence spectroscopy indicate that the transitions $B^1\Pi \rightarrow a^3\Sigma^+$ and $D^1\Pi \rightarrow a^3\Sigma^+$ give the evidence of the mixing of the singlet excite state and triplet excite state [3, 18–20].

II. CALCULATION MODEL AND METHOD

In this work, the pseudopotential model based on the core-polarization modification and the *ab initio* method is adopted. The pseudopotential model is used to simplify the atom of Z nuclear charges and N electrons to the equivalent system of N_v ($=N-n_{core}$) valence electrons and ($Z-n_{core}$) core nuclear charges, in which the core is served as a chemical stable unit and its affection on the valence electrons is described by the nonlocal (independent of the principal quantum number n and azimuthal quantum number l) or semilocal (only dependent of the azimuthal quantum number l) form. In contrast to the full electron quantum chemical calculation, the pseudopotential model losses the calculation accuracy generally, especially resulting in the large uncertainty for the core-polarization effect. Thus, including the core-polarization can describe the core-valence electron interaction more accurately, and decrease the uncertainty from the core frozen model. The core-polarization modification of pseudopotential model includes the polarization terms arising from the core-valence electron inter-attraction and core-core mutual interaction, which gives a preferable description of polarization effect between the core and valence electron and affection on the valence electron from the electric field generated by certain core and the interaction from all other cores.

When the pseudopotential model is used to describe the potentials of valence electron-valence electron, valence electron-core, and core-core, the core itself cannot be served as an ideal particle, but a circle with a radius r_{core}. When the distance r between the valence electron and the core is smaller than the radius r_{core} of the core, the potential terms need to be truncated. There are two general approximation methods: (i) to multiply each potential term by a cutoff function $(1-e^{-(r/\rho)^2})$

DOI:10.1063/1674-0068/cjcp1904065

or quadratic term (the cutoff parameter ρ is applied to the electron of different angular momentum), which can make the potential energy term of the valence electron-valence electron and the valence electron-core quickly attenuate to zero; (ii) to set the cutoff function as a segmented function, that is, when $r \leq r_{\rm core}$, the value of the cutoff function is set as zero, when $r > r_{\rm core}$, the cutoff function is set with different ρ_λ parameters according to the angular momentum of the electron. The former study indicates that the uncertainty of the single cutoff parameter method will increase significantly with the intensity of the core-polarization. To the light alkali atom, the uncertainty of the single cutoff parameter method will be rather small. For example, the uncertainties of the calculations with the single cutoff parameter method about the transitions ^{2}P$\rightarrow^2$S of Li, Na, and K atoms are only 20 cm^{-1}, 44 cm^{-1}, and 20 cm^{-1}, respectively. However, the uncertainty with the single cutoff parameter method applied in the calculations of the heavy alkali atom will become quite large. The extrapolation uncertainty from Stevens's calculations [21] comes up to 220 cm^{-1}. In order to keep the accuracy and simplify the calculation as much as possible, the single cutoff parameter method will be adopted in the present work.

After describing the molecular system with the core-polarization modification pseudopotential model, the PECs of the exited states need to be derived with the quantum chemical calculation method. In the present work, the full valence CI reference with intrinsic contraction is applied to calculate the PECs of the 10 electronic states correlated with the three lowest dissociation limits, and the quantum chemical calculations are accomplished in the MOLPRO 2010 package [22]. The ECP10SDF and ECP18SDF are employed to describe the structure of the pseudopotential of Na and K atoms. The basis wave function of Na atom contains s, p, and d component, and the s component and p component use generalized homogenous adjustment functions. The final basis wave functions include 8 s functions (23.382686, 7.794229, 2.598076, 0.866025, 0.288675, 0.096225, 0.032075, and 0.010692), 6 p functions (3.117691, 1.039230, 0.346410, 0.115470, 0.038490, and 0.012830), and 2 d functions (0.12, and 0.03).

The calculation of the matrix element of the core-polarization is employed with the CPP subroutine in the MOLPRO program package, in which the core dipole polarizabilities of the Na and K atom $\alpha_{\rm Na}$ and $\alpha_{\rm K}$ are 0.9947 a$_0$ and 5.354 a$_0$, respectively. The exponents of the cutoff parameter $(1/\rho_{\rm Na})^2$ and $(1/\rho_{\rm K})^2$ are 0.62 and 0.29 respectively. Due to the adoption of the effective potential energy of the single valence electron, the number of the valence electron in the whole molecular system is only 2, and thus the highest precision full valence CI method can be applied [23, 24]. In the optimization of the wave function of the full valence CI method, the $^1\Sigma^+$, $^3\Sigma^+$, $^1\Pi$, and $^3\Pi$ states are chosen to do the energy scanning in the internuclear distance range of 2.5−20 Bohr. After obtaining the PECs of the electronic states, LEVEL procedure [25] is adopted to obtain the eigenvalue and eigenfunction of the bound state and the Frank-Condon factor for a pair of two states.

TABLE I The energy gap between different dissociation limits of NaK. The lowest dissociation limit is Na(3s)+K(4s).

Dissociation limit	Energy gap/cm^{-1}	
	This work	Expt.[26]
Na(3s)+K(4s)	0	0
Na(3s)+K(4p)	13014	13024
Na(3p)+K(4s)	16955	16968

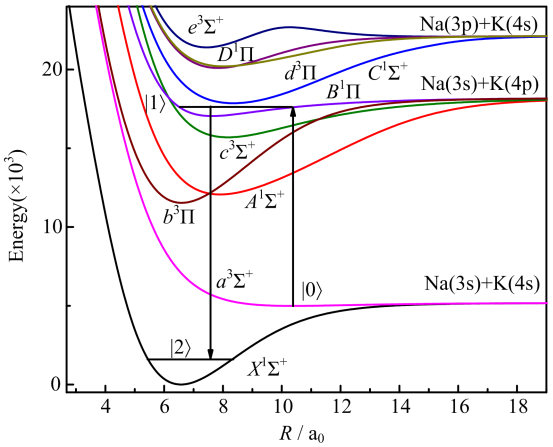

FIG. 1 Potential energy curves of low-lying Λ-S states of NaK computed by configuration interaction method with pseudopotential basis set.

III. RESULTS AND DISCUSSION

A. Electronic structure and spectroscopic properties of Λ-S states of NaK

The dissociation relationships are presented in Table I. The calculated energy separations with respect to the ground-state dissociation limit (Na(3s)+K(4s)) are 13014 cm^{-1} and 16955 cm^{-1}, respectively, which are ∼10 cm^{-1} lower than the experimental data [26]. The PECs of the 10 Λ-S states are plotted in FIG. 1. Spectroscopic constants for the 10 Λ-S states are evaluated and listed in Table II. Our calculation results agree well with known experimental data and other theoretical results: the differences between our computation and existing experimental results are 0.01−0.10 a$_0$, 50−100 cm^{-1}, 2−4 cm^{-1}, and 20−150 cm^{-1} for $R_{\rm e}$, $T_{\rm e}$, $\omega_{\rm e}$, and $D_{\rm e}$, respectively. It should be noted [27] that semi-empirical pseudopotentials give systematically shorter equilibrium nuclear distances than experimental values. To make the PECs more convenient for further applications, we give the analytical poten-

DOI:10.1063/1674-0068/cjcp1904065

TABLE II Spectroscopic constants of bound states of NaK. Previous theoretical and experimental values are also listed for comparison.

Electronic state		R/a_0	T_e/cm^{-1}	ω_e/cm^{-1}	D_e/cm^{-1}
$X^1\Sigma^+$	Expt. [32]	6.61	0	124.01	5275
	Calc. [18]	6.57	0	123.44	5187
	This work	6.57	0	122.67	5181
$a^3\Sigma^+$	Expt. [32]	10.28	5066	22.99	209
	Calc. [18]	10.23	4996	22.63	197
	This work	10.38	4990	20.68	192
$b^3\Pi$	Expt. [32]	6.62	11562	120.41	6737
	Calc. [18]	6.57	11507	120.06	6709
	This work	6.59	11537	119.42	6659
$A^1\Sigma^+$	Expt. [32]	7.93	12137	81.25	6220
	Calc. [18]	7.89	12089	81.00	6122
	This work	7.90	12070	79.96	6126
$c^3\Sigma^+$	Expt. [32]	8.14	15669	73.40	2541
	Calc. [18]	8.10	15678	73.42	2538
	This work	8.17	15697	71.07	2498
$B^1\Pi$	Expt. [32]	7.58	16993	71.46	1305
	Calc. [18]	7.63	17023	68.91	1193
	This work	7.63	17048	64.09	1148
$C^1\Sigma^+$	Expt. [32]	8.40	17787	69.66	4455
	Calc. [18]	8.35	17846	68.74	4314
	This work	8.35	17864	67.55	4272
$D^1\Pi$	Expt. [32]	7.92	20093	81.52	2149
	Calc. [18]	7.82	20087	83.71	2073
	This work	7.83	20102	81.12	2034
$d^3\Pi$	Expt. [32]	7.98	20248	67.38	2012
	Calc. [18]	7.98	20195	66.18	1965
	This work	8.02	20205	64.47	1931
$e^3\Sigma^+$	Expt. [32]	7.44	21380	94.20	774
	Calc. [18]	7.44	21386	93.80	774
	This work	7.43	21410	93.01	726

tial energy function for the $X^1\Sigma^+$, $A^1\Sigma^+$, $b^3\Pi$, $B^1\Pi$, and $a^3\Sigma^+$ states of NaK. The expression for analytical potential energy function can be written as

$$V(R) = A_0 + A_1R + A_2R_2 + A_3R_3 + A_4R_4 + A_5R_5 \quad (1)$$

The fitted parameters and residual mean square of the analytical potential energy function are listed in Table III.

The recent experimental production of ground-state ultracold polar fermionic NaK molecule comes from weakly bound Feshbach molecule/Fano-Feshbach resonance with mixture of the singlet $X^1\Sigma^+$ and triplet $a^3\Sigma^+$ states. The dominant component of the Fano-Feshbach resonance state is the corresponding quantum state of the highest bound state of the lowest-excited triplet ground state. Therefore, we can check in detail the accuracy of our calculations to compare our $a^3\Sigma^+$ PEC with those known at large internuclear distances. As shown in FIG. 1, based on the asymptotic behavior for PECs of the singlet $X^1\Sigma^+$ and triplet $a^3\Sigma^+$ states and the semiclassical method (WKB), theoretical calculations can provide information about the maximum vibrational quantum state of the singlet and triplet ground states [28]. Table IV lists the vibrational quantum number of the maximum bound state of the $X^1\Sigma^+$ and $a^3\Sigma^+$ states of the three isotopes of the NaK molecules. The maximum vibrational quantum number of the bound state of $^{23}Na^{39}K$ is calculated to be 19, which is in good agreement with the high-resolution observation [30].

After the confirmation of the Fano-Feshbach resonance state, a proper resonant singlet-triplet coupling of the intermediate levels must be chosen to overcome the singlet-triplet transfer prohibition and efficient transfer of ultracold NaK molecules from the Na(3s)+K(4s) asymptote to the lowest levels of the ground state. In order to guarantee high-efficiency transfer to the absolute rovibrational ground state from a weakly bound Feshbach molecules via a coherent two-photon transfer, criteria for the intermediate state $|e\rangle$ are: (i) the intermediate state must feature strong singlet-triplet mixing because the initial Feshbach molecular state is dominantly associated with the triplet state ($a^3\Sigma^+$ for NaK), so the intermediate state can strongly connect the initial Feshbach molecular state to the absolute rovibrational singlet ground state; (ii) both TDMs of the intermediate state coupling with the Feshbach molecular state and the absolute ground state should be large, it means the Franck-Condon overlap between the states is significant if the TDMs are close to be constant for both the initial Feshbach molecular state to the intermediate state and the intermediate state to the singlet ground state transitions; (iii) vibrational levels of the mixed complex potentials are close enough to display significant singlet-triplet mixing, intermediate states chosen by Zwierlein group [14] are [$B^1\Pi$, $c^3\Sigma^+$]-system. Therefore, we calculated the probable mixing ranges between the vibrational levels of the two electronic states based on the energy of the first 40 vibrational levels (v=0−39) of the $B^1\Pi$ and $c^3\Sigma^+$ states. Thus, the wavelengths of the two lasers ω_1 and ω_2 in the two-photon STIRAP are estimated. As displayed in Table V, our calculation results provide the absolute energy position of the vibrational levels of the $a^3\Sigma^+$, $B^1\Pi$, and $c^3\Sigma^+$ states of NaK molecule. Our calculation results predict that the v=0 vibrational level (17056.8 cm^{-1}) of the $B^1\Pi$ state is close to the v=22 (17056.4 cm^{-1}) of the $c^3\Sigma^+$ state, and the v=14 vibrational level (17712.4 cm^{-1}) of the $B^1\Pi$ state is near the convergence limit of the v=39 vibrational levels (17719.5 cm^{-1}) of the $c^3\Sigma^+$ state. Thus, the mixing range of the two electronic states is v=22−39 of $c^3\Sigma^+$ and v=0−14 of $B^1\Pi$ state. In fact, Zwierlein *et al.* [13] chose the resonantly mixed complex for v=35 of $c^3\Sigma^+$ to v=12 of $B^1\Pi$. Therefore, the wavelength ranges for the two lasers ω_1 and ω_2 are estimated as

DOI:10.1063/1674-0068/cjcp1904065

TABLE III Fitted parameters and residual mean square of the analytical potential energy functions for the $X^1\Sigma^+$, $A^1\Sigma^+$, $b^3\Pi$, $B^1\Pi$, and $a^3\Sigma^+$ states of NaK.

	A_0	A_1	A_2	A_3	A_4	A_5	Residual mean square
$X^1\Sigma^+$	107.51745	−47.43524	7.85617	−0.60802	0.02245	-3.20048×10^{-4}	0.13095
$A^1\Sigma^+$	111.23268	−36.27029	4.9293	−0.3113	0.00935	-1.07986×10^{-4}	0.09154
$b^3\Pi$	123.91354	−50.09891	8.33042	−0.64421	0.02375	-3.38109×10^{-4}	0.03482
$B^1\Pi$	122.96173	−43.56298	6.87116	−0.52116	0.01915	-2.74127×10^{-4}	0.06695
$a^3\Sigma^+$	103.31817	−37.04792	5.43861	−0.3896	0.01365	-1.8767×10^{-4}	0.03071

Note: the expression for analytical potential energy function is written as Eq.(1).

TABLE IV The number of vibrational levels of $X^1\Sigma^+$ and $a^3\Sigma^+$ state. Previous theoretical and experimental values are also listed for comparison.

	This work		Calc. [29]		Expt. [30]	
	$X^1\Sigma^+$	$a^3\Sigma^+$	$X^1\Sigma^+$	$a^3\Sigma^+$	$X^1\Sigma^+$	$a^3\Sigma^+$
Na^{23}-K^{39}	74	19	74	19	73	19
Na^{23}-K^{40}	74	20	74	19		
Na^{23}-K^{41}	74	20	74	20		

TABLE V $G(v)$ value of $a^3\Sigma^+$, $B^1\Pi$, and $C^3\Sigma^+$. v is vibrational quantum number of bound states.

v	$G(v)/\mathrm{cm}^{-1}$			v	$G(v)/\mathrm{cm}^{-1}$	
	$a^3\Sigma^+$	$C^3\Sigma^+$	$B^1\Pi$		$C^3\Sigma^+$	$B^1\Pi$
0	5086.6	15739.8	17056.87	20	16957.1	17882.4
1	5105.9	15809.6	17118.2	21	17007.3	17905.6
2	5124.1	15878.6	17177.1	22	17056.4	17927.4
3	5140.9	15946.7	17233.5	23	17104.5	17947.7
4	5156.5	16013.9	17287.6	24	17151.4	17966.8
5	5170.8	16080.1	17339.4	25	17197.3	17984.5
6	5183.8	16145.4	17389.0	26	17242.0	18000.9
7	5195.6	16209.8	17436.4	27	17285.6	18016.0
8	5206.0	16273.2	17481.6	28	17328.1	18029.8
9	5215.2	16335.7	17524.8	29	17369.4	18042.3
10	5223.0	16397.2	17566.0	30	17409.6	18053.6
11	5229.7	16457.8	17605.3	31	17448.7	18063.7
12	5235.1	16517.3	17642.8	32	17486.5	18072.6
13	5239.3	16575.9	17678.4	33	17523.3	18080.3
14	5242.4	16633.4	17712.4	34	17558.9	18086.9
15	5244.5	16690.0	17744.6	35	17593.3	18092.4
16	5245.8	16745.5	17775.2	36	17626.6	18097.0
17	5246.5	16799.9	17804.3	37	17658.7	18100.6
18	5246.8	16853.4	17831.8	38	17689.7	18103.3
19	5246.9	16905.7	17857.9	39	17719.5	18105.3

800−847 nm and 564−586 nm respectively, while the laser wavelengths used in the experiment of Zwierlein *et al.* [13] are 804.7 and 566.9 nm. Our calculation results agree with the experimental parameters for the ultracold alkali diatomic molecular experiment.

The dipole moments (DMs) of the 10 Λ-S states are computed with CI method. The DMs of the 10 Λ-S states are displayed in FIG. 2. At the bond length R=6.61 a_0, the DM of the $X^1\Sigma^+$ is computed to be 1.16 a.u., which is in good consistence with experimental result of 1.05 a.u. [31] . The positive value of the DM of the $X^1\Sigma^+$ indicates the $Na^{\delta-}K^{\delta+}$ polarity of the molecule. At the correspond equilibrium distance of $A^1\Sigma^+$, $C^1\Sigma^+$ and $B^1\Pi$, the DMs are calculated to be 0.03 a.u., 0.68 a.u. and −1.28 a.u., which agree with existing theoretical results of 0.02 a.u., 0.67 a.u. and −1.27 a.u. As depicted in FIG. 2, the DMs of the 10 Λ-S states tend to be zero as $R\to\infty$, illuminating that the dissociation products are neutral Na and K atom.

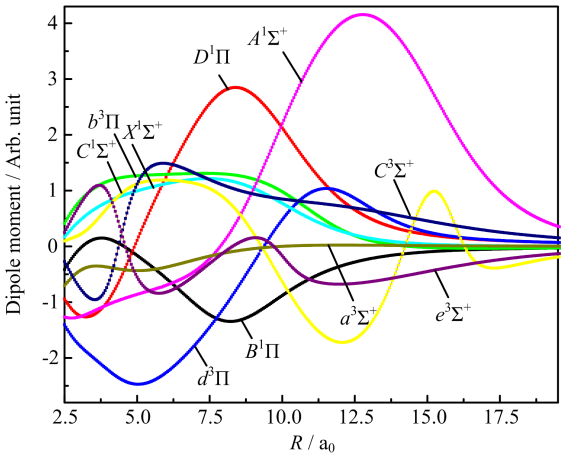

FIG. 2 Permanent dipole moment curves of low-lying Λ-S states of NaK as function of internuclear distance.

B. Transition properties and lifetimes

The TDMs between excited singlet and the ground state are computed by CI level of theory. The TDMs curves of $C^1\Sigma^+$-$X^1\Sigma^+$, $A^1\Sigma^+$-$X^1\Sigma^+$, and $B^1\Pi$-$X^1\Sigma^+$ transitions are plotted in FIG. 3. At the equilibrium distance (R=7.63 Å) of $B^1\Pi$ state, the absolute value of TDM of $B^1\Pi$-$X^1\Sigma^+$ transition is calculated to be 2.5 a.u., which is 0.4 a.u. smaller than previously available theoretical value of 2.9 a.u. [33]. As show in FIG. 3, the absolute values of TDMs of $A^1\Sigma^+$-$X^1\Sigma^+$ and $B^1\Pi$-

DOI:10.1063/1674-0068/cjcp1904065

TABLE VI Franck-Condon factors (FCFs) and energy gap $\Delta E_{v'v''}$ for the $A^1\Sigma^+$-$X^1\Sigma^+$, $C^1\Sigma^+$-$X^1\Sigma^+$, and $B^1\Pi$-$X^1\Sigma^+$ transitions of NaK. v' is initial vibrational level, v'' is the final vibrational level.

		v''=0		v''=1		v''=2	
	v'	FCFs	$\Delta E_{v'v''}/\mathrm{cm}^{-1}$	FCFs	$\Delta E_{v'v''}/\mathrm{cm}^{-1}$	FCFs	$\Delta E_{v'v''}/\mathrm{cm}^{-1}$
$A^1\Sigma^+$-$X^1\Sigma^+$	0	2.51×10^{-5}	12052.79	3.14×10^{-4}	11929.98	1.91×10^{-3}	11808.22
	1	2.19×10^{-4}	12132.84	2.25×10^{-3}	12010.03	1.09×10^{-2}	11888.27
	2	9.92×10^{-4}	12212.42	8.26×10^{-3}	12089.60	3.12×10^{-2}	11967.85
$C^1\Sigma^+$-$X^1\Sigma^+$	0	3.90×10^{-8}	17842.54	7.85×10^{-7}	17719.73	7.80×10^{-6}	17597.97
	1	5.60×10^{-7}	17910.17	1.00×10^{-5}	17787.35	8.71×10^{-5}	17665.60
	2	4.10×10^{-6}	17977.80	6.46×10^{-5}	17854.99	4.90×10^{-4}	17733.23
$B^1\Pi$-$X^1\Sigma^+$	0	1.60×10^{-3}	17025.51	1.03×10^{-2}	16902.70	3.34×10^{-2}	16780.94
	1	7.72×10^{-3}	17089.67	3.73×10^{-2}	16966.86	8.45×10^{-2}	16845.10
	2	2.00×10^{-2}	17151.32	7.05×10^{-2}	17028.51	1.04×10^{-1}	16906.75

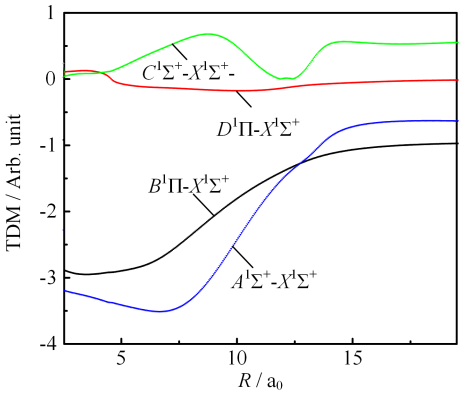

FIG. 3 Transition dipole moment of spin-allowed transitions $A^1\Sigma^+$-$X^1\Sigma^+$, $C^1\Sigma^+$-$X^1\Sigma^+$, $B^1\Pi$-$X^1\Sigma^+$, and $D^1\Pi$-$X^1\Sigma^+$.

$X^1\Sigma^+$ are obviously larger than that of $C^1\Sigma^+$-$X^1\Sigma^+$. On the basis of the calculated PECs of $X^1\Sigma^+$, $C^1\Sigma^+$, $A^1\Sigma^+$, and $B^1\Pi$, the Franck-Condon factors (FCFs) and energy gap $\Delta E_{v'v''}$ for the $A^1\Sigma^+$-$X^1\Sigma^+$, $C^1\Sigma^+$-$X^1\Sigma^+$ and $B^1\Pi$-$X^1\Sigma^+$ transitions are calculated and given in Table VI.

On the basis of the calculated TDMs, vibrational levels and FCFs, the radiative lifetimes of bound state is evaluated by the following formula

$$\tau = \left(\sum_{v''} A_{v'v''}\right)^{-1} \tag{2}$$

where $A_{v'v''}$ is Einstein coefficient of vibrational levels v' and v''. $A_{v'v''}$ [34] is defined by

$$\begin{aligned} A_{v'v''} &= \frac{64\pi^4 q_{v'v''}|\mathrm{a_0}\cdot\mathrm{e}\cdot\mathrm{TDM}|^2\Delta E^3_{v'v''}}{3h} \\ &= 2.026\times10^{-6}\left(q_{v'v''}|\mathrm{TDM}|^2\Delta E^3_{v'v''}\right) \end{aligned} \tag{3}$$

where $q_{v'v''}$ is the FCF of two vibrational states v' and v'', TDM (in atomic unit) is the average TMD between classical turning points of v' vibrational state, $\Delta E_{v'v''}$ (in unit of cm^{-1}) is the energy gap between vibrational states v' and v''.

TABLE VII Lifetime of the six low-lying vibrational states of $A^1\Sigma^+$, $C^1\Sigma^+$, and $B^1\Pi$ state. The previous experimental results are also given for comparison.

v'	Radiative lifetime/nm			
	$A^1\Sigma^+$	$C^1\Sigma^+$	$B^1\Pi$	Expt. [35]
0	33.4	250.0	18.6	
1	33.5	250.0	19.0	13.4
2	33.6	250.0	19.4	14.3
3	33.7	250.0	19.8	13.5
4	33.8	249.9	20.1	14.8
5	33.8	249.9	20.6	14.9

Table VII lists the radiative lifetime of the excited states $A^1\Sigma^+$, $B^1\Pi$ and $C^1\Sigma^+$, and also lists the experimentally estimated lifetimes of low-lying vibrational states of $B^1\Pi$ [35]. For the v'=1, v'=2, v'=3, v'=4, and v'=5 vibrational levels of $B^1\Pi$, the lifetime is computed to be 19.0, 19.4, 19.8, 20.1, and 20.6 ns, which agrees with experimental values of 13.4, 14.3, 13.5, 14.8, and 14.9 ns [35]. The calculated lifetimes of $B^1\Pi$ and $A^1\Sigma^+$ are on the order of 10 ns, while lifetime of $C^1\Sigma^+$ is one order of magnitude larger than those of $B^1\Pi$ and $A^1\Sigma^+$ states.

IV. CONCLUSION

The PECs of the 10 Λ-S states of the NaK molecule correlated with the asymptotes of Na(3s)+K(4s), Na(3s)+K(4p), and Na(3p)+K(4s), have been computed with the *ab initio* method. On the basis of our calculated PECs, the spectroscopic constants of the bound states are evaluated, which are in good agreement with existing experimental results. The maximum vibrational quantum numbers of the bound level

DOI:10.1063/1674-0068/cjcp1904065

of the singlet ground state $X^1\Sigma^+$ and the triplet ground state $a^3\Sigma^+$ have been calculated for the three isotopes $^{23}Na^{39}K$, $^{23}Na^{40}K$, and $^{23}Na^{41}K$, and analyzed with the semiclassical scattering theory, which agrees well with the experimental observations on $^{23}Na^{39}K$. The accurate DM curves and TDM curves of low-lying Λ-S states are computed at level of CI level. Based on the calculated TDMs, FCFs, and vibrational levels, the lifetimes of $B^1\Pi$ are determined, which are found to be in reasonable agreement with experimental results. The mixed vibrational levels between the $c^3\Sigma^+$ and $B^1\Pi$ states have been analyzed according to the PECs of current theoretical calculations, and the laser wavelengths for the STIRAP process have been deduced, which can shed light on the formation of ultracold NaK molecular experiment.

V. ACKNOWLEDGEMENTS

This work was supported by the National Key Research and Development Program of China (No.2017YFA0304900, No.2017YFA0402300, and No.2016YFA0300600), the Strategic Priority Research Program of Chinese Academy of Sciences (No.XDB28000000 and No.XDB07030000), the National Natural Science Foundation of China (No.11604334, No.11575099 and No.11474347), the Open Research Fund Program of the State Key Laboratory of Low-Dimensional Quantum Physics (No.KF201807) and the Science Challenge Project (No.TZ2016005). Fruitful discussions with Prof. Jie Ma at State Key Laboratory of Quantum Optics and Quantum Optics Devices, Laser Spectroscopy Laboratory, Shanxi University, are gratefully acknowledged.

[1] G. Quéméner and P. S. Julienne, Chem. Rev. **112**, 4949 (2012).
[2] J. Baron, W. C. Campbell, D. DeMille, J. M. Doyle, G. Gabrielse, Y. V. Gurevich, P. W. Hess, N. R. Hutzler, E. Kirilov, and I. Kozyryev, Science **343**, 269 (2014).
[3] D. DeMille, S. Sainis, J. Sage, T. Bergeman, S. Kotochigova, and E. Tiesinga, Phys. Rev. Lett. **100**, 043202 (2008).
[4] T. Zelevinsky, S. Kotochigova, and J. Ye, Phys. Rev. Lett. **100**, 043201 (2008).
[5] D. DeMille, Phys. Rev. Lett. **88**, 067901 (2002).
[6] L. D. Carr, D. DeMille, R. V. Krems, and J. Ye, New J. Phys. **11**, 055049 (2009).
[7] M. A. Baranov, M. Dalmonte, G. Pupillo, and P. Zoller, Chem. Rev. **112**, 5012 (2012).
[8] K.K. Ni, S. Ospelkaus, M. De Miranda, A. Pe'Er, B. Neyenhuis, J. Zirbel, S. Kotochigova, P. Julienne, D. Jin, and J. Ye, Science **322**, 231 (2008).
[9] H. Yang, D. C. Zhang, L. Liu, Y. X. Liu, J. Nan, B. Zhao, and J. W. Pan, Science **363**, 261 (2019)
[10] T. Hartmann, T. A. Schulze, K. K. Voges, P. Gersema, M. W. Gempel, E. Tiemann, A. Zenesini, and S. Ospelkaus, Phys. Rev. A **99**, 032711(2019)
[11] A. Viel and A. Simoni, Phys. Rev. A **93**, 042701 (2016).
[12] I. Temelkov, H. Knöckel, A. Pashov, and E. Tiemann, Phys. Rev. A **91**, 032512 (2015).
[13] J. W. Park, S. A. Will, and M. W. Zwierlein, Phys. Rev. Lett. **114**, 205302 (2015).
[14] W. Müller and W. Meyer, J. Chem. Phys. **80**, 3311 (1984).
[15] G. H. Jeung, J. P. Daudey, and J. P. Malrieu, Chem. Phys. Lett. **94**, 300 (1983).
[16] G. H. Jeung, Phys. Rev. A **35**, 26 (1987).
[17] G. H. Jeung and A. J. Ross, J. Phys. B **21**, 1473 (1988).
[18] S. Magnier and P. Millié, Phys. Rev. A **54**, 204 (1996).
[19] S. Magnier, M. Aubert-Frécon, and P. Millié, J. Mol. Spectrosc. **200**, 96 (2000).
[20] I. Russier-Antoine, A. J. Ross, M. Aubert-Frécon, F. Martin, and P. Crozet, J. Phys. B **33**, 2753 (2000).
[21] W. J. Stevens, D. D. Konowalow, and L. B. Ratcliff, J. Chem. Phys. **80**, 1215 (1984).
[22] H. J. Werner, P. J. Knowles, G. Knizia, F. R. Manby, M. Schütz, P. Celani, T. Korona, R. Lindh, A. Mitrushenkov, and G. Rauhut, *MOLPRO: a Package of ab initio Programs*, See http://www. molpro. net, (2010).
[23] H. J. Werner and P. J. Knowles, J. Chem. Phys. **89**, 5803 (1988).
[24] P. J. Knowles and H. J. Werner, Chem. Phys. Lett. **145**, 514 (1988).
[25] R. J. Le Roy, *LEVEL 8.0: A Computer Program for Solving the Radial Schrödinger Equation for Bound and Quasibound Levels*, (University of Waterloo Chemical Physics Research Report CP-663), (2007).
[26] C. E. Moore, *Atomic Energy Levels*, Washington, DC: National Bureau of Standard, (1971).
[27] P. Fuentealba, H. Preuss, H. Stoll, and L. Von-Szentpály, Chem. Phys. Lett. **89**, 418 (1982)
[28] K. Ishikawa, N. Mukai, and M. Tanimura, J. Chem. Phys. **101**, 876 (1994).
[29] A. Gerdes, M. Hobein, H. Knöckel, and E. Tiemann, Eur. Phys. J. D **49**, 67 (2008).
[30] K. Ishikawa, N. Mukai, and M. Tanimura J. Chem. Phys. **101**, 876, (1994).
[31] P. J. Dagdigian and L. Wharton, J. Chem. Phys. **57**, 1487 (1972).
[32] A. J. Ross, C. Effantin, J. d'Incan, and R. F. Barrow, Mol. Phys. **56**, 903 (1985).
[33] M. Tamanis, M. Auzinsh, I. Klincare, O. Nikolayeva, R. Ferber, A. Zaitsevskii, E. A. Pazyuk, and A. V. Stolyarov, J. Chem. Phys. **109**, 6725 (1998).
[34] H. Okabe, *Photochemistry of Small Molecules*, New York: Wiley-Interscience, (1978).
[35] J. Derouard, H. Debontride, T. D. Nguyen, and N. Sadeghi, J. Chem. Phys. **90**, 5936 (1989).

DOI:10.1063/1674-0068/cjcp1904065